Int. J. Electrochem. Sci., 12 **(2017)** 6622 – 6637, doi: 10.20964/2017.07.29

International Journal of
ELECTROCHEMICAL
SCIENCE
www.electrochemsci.org

Molecular Dynamics Simulation of Adsorption Behavior of Schiff base Gemini Surfactants on Zn (1 1 0) Surface

Haiying Li[1], *Zheng Liu*[1,*], *Hao Wang*[1], *Guo-Cheng Han* [2,*], *Yong Zhao*, *Si-wei Xie* [1], *Shufen Zhang*[1], *Zhencheng Chen*[2], *Shuang Li*[2]

[1]Chemistry and Biological Engineering, Guilin University of Technology, Guilin, 541004, P.R. China
[2]School of Life and Environmental Sciences, Guilin University of Electronic Technology, Guilin 541004, P.R. China
[*]E-mail: lisa4.6@163.com, hangc1981@163.com

Received: 12 March 2017 / *Accepted:* 27 April 2017 / *Published:* 12 June 2017

Molecular dynamics simulation method was selected to investigate the adsorption behavior of three quaternary ammonium Schiff base Gemini surfactants on Zn (1 1 0) surface, including 4,4'-(hydrazine-1,2-diylidenebis-(methanylylidene))bis-(N-decyl-N,N-dimethylbenzenaminium)bromide(D1),4,4'-(hydrazine-1,2-diylidenebis(methanylylidene))bis(N-dodecyl-N,N-dimethylbenzenaminium) bromide (D2), and 4,4'-(hydrazine-1,2-diylidenebis(methanylylidene))bis(N-myristyl-N,N-dimethylbenzen-aminium)bromide(D3). The electrochemical impedance spectroscopy (EIS) and scanning electron microscope (SEM) showed that D3 had better corrosion inhibition performance for the zinc electrode and more excellent inhibitory effect on dendrite, deformation and passivation of zinc. The molecular dynamics simulation results indicated that the order of adsorption energy of three Schiff base Gemini surfactants was D3>D2>D1, the adsorption rate followed the order of D3 >D2 > D1. The adsorption energy was greater and the adsorption rate was faster, D3 had the best effect on corrosion inhibition, inhibiting dendrite and deformation.

Keywords: Schiff base Gemini surfactants; molecular dynamics simulation; adsorption behavior; corrosion inhibition

1. INTRODUCTION

Recently, the corrosion resistance of metals has become a hot topic [1]. The corrosion inhibitors can prevent metal corrosion when the metals form a dense layer of adsorption film [2]. The mechanism of action is closely related to the type of inhibitor, the type of inhibitor is different, and their mechanism is disparate [3].

Recent studies have indicated that Gemini surfactants can be used as corrosion inhibitor. D. Gelman and co-workers studied the correlation between Al corrosion rates and the concentrations of both PEG di-acid and ZnO in alkaline solution [4]. A. A. Mohamad and co-workers studied poly(vinyl alcohol) alkaline solid polymer in KOH solution, the results showed that the corrosion inhibitor can significantly reduce the corrosion of zinc electrode [5]. H. Yang and co-workers suppressed surface passivation of zinc anode in dilute alkaline solution using surfactant additives, which increased the discharge capacity of zinc battery [6]. W.L. Chang and co-workers studied the behavior of zinc anodes in presence of inhibitors, the results revealed that these inhibitors can improve the over- potential of hydrogen evolution and decrease the formation of zinc dendrite [7]. H.M.A. El-Lateef and co-workers studied the effect of inhibitors on carbon steel, such as CHOGS-8, CHOGS-12 and CHOGS-16 in 15% HCl solution, the results showed that the prepared surfactants were effectively inhibited the carbon steel corrosion [8]. The research on interaction between a family of Gemini amphiphilic pseudopeptides and model monomolecular film membranes [9] had aided in elucidating the role of surfactant structure in the CNT dispersion process, and reported the results of fully atomistic molecular dynamics (MD) simulations of the adsorption and surface self-assembly of Gemini surfactants [10].

Materials Studio was designed for materials science and structural chemistry. The emergence of Materials Studio, many important problems are solved in pharmaceuticals, catalysts, polymers & composites, metals & alloys, batteries & fuel cells [11-14]. Also, Material Studio was used for simulating and calculating the adsorption performance and mechanism of corrosion inhibitor [15-19]. The physical and chemical behavior of organic corrosion inhibitor molecules on the metal surface was expressed [20]. The microscopic particle process of inhibitor molecules' adsorption on the metal surface, bonding and filming was explained [21, 22]. And Material Studio provided sufficient conditions for further exploring the inhibition mechanism and the relationship between structure and function of corrosion inhibitor [23-25].

In this paper, molecular dynamics simulation method was selected to investigate the adsorption behavior of three quaternary ammonium Schiff base Gemini surfactants on Zn (1 1 0) surface, including 4,4'-(hydrazine-1,2-diylidenebis (methanylylidene))bis(N-decyl-N,N-dimethylbenzen-aminium)bromide(D1), 4,4'-(hydrazine-1,2-diylidenebis(methanylylidene))bis(N-dodecyl-N,N-dimethylbenzenaminium)bromide(D2), and 4,4'-(hydrazine-1,2-diylidenebis(methanylylidene)) bis(N-myristyl-N,N-dimethylbenzenaminium)bromide(D3). The corrosion inhibition performance of these three Schiff base Gemini surfactants were investigated experimentally, using measurements based on EIS and SEM. The Material Studio 5.5 software was adopted to investigate its absorption behavior on Zn (1 1 0) surface in aqueous solution, as well as adsorption mechanism. And studying of adsorption performance will provide theoretical basis for the design and synthesis of the Schiff base surfactants.

2. COMPUTATIONAL METHODS

The absorption behavior on Zn (1 1 0) surface in aqueous solution and its adsorption mechanism of the three Schiff base Gemini surfactants was carried out using a commercial software package called Materials Studio 5.5 developed by Accelrys Inc.

2.1. Calculation model building

The molecular structure models of three Schiff base Gemini surfactants (D1, D2, D3) were draw using Materials Studio5.5, as shown in Fig.1.

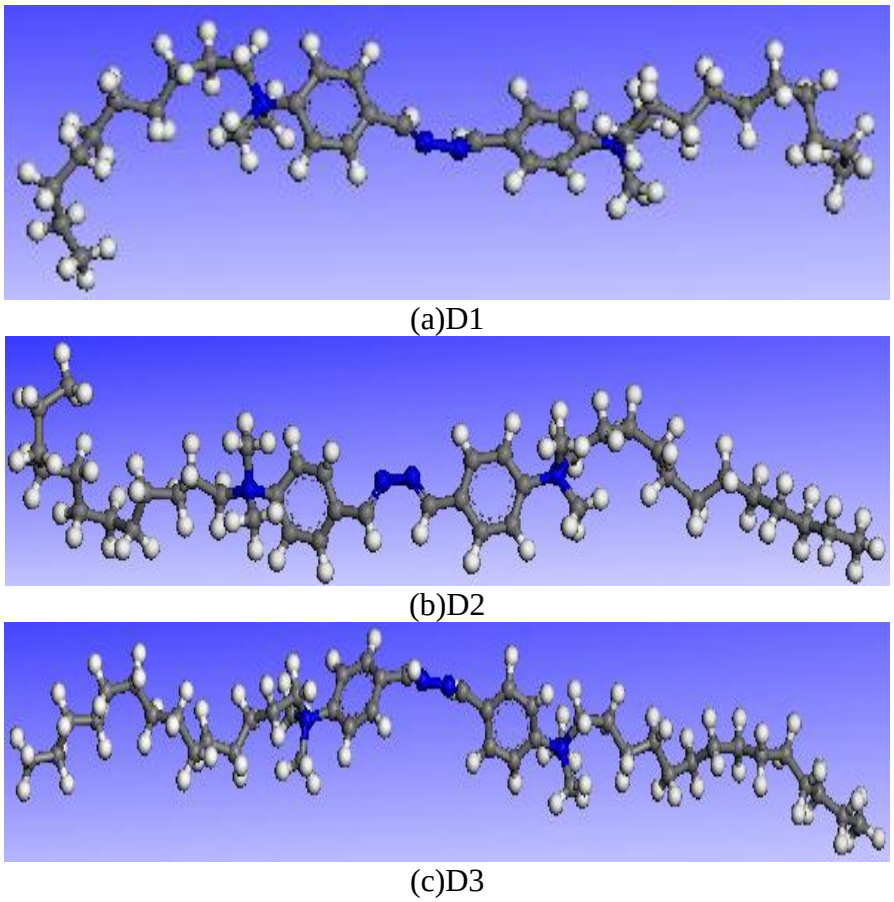

Figure 1. (a) The molecular structure model of D1; (b) The molecular structure model of D2; (c) The molecular structure model of D3

The whole simulation system consists of three layers, including Zn (1 1 0) surface, the solution layer containing Schiff base Gemini surfactant molecules and water molecules, and the solution layer only containing water molecules. Here are the steps for drawing the structure model. First, Zn (110) surface was established by using pure metal Zn lattice of Import software. Second, open the Surface-Cleave Surface option in the Build module, and then input 110 in the Cleave plane (h k l), Zn (110) surface is cut into 8 layers. Third, the supercell containing 2304 Zn atoms [26] is established by utilizing Build-Symmetry-Supercell option. Fourth, Zn supercell is optimized by using the same method, all atomic coordinates of Zn (110) surface is fixated after checking Modify-Constraints-Fix Cartesian position option. Fifth, click the Construction on Amorphous Cell menu to establish two aqueous solution layers. The one contains 2000 water molecules, and the system size is 56×56×19.66 Å. The other one contains 1000 water molecules, and the system size is 56×56×9.83 Å. Sixth, Select the layer of water molecules, and then check the Modify-Constraints-Fix Cartesian position option.

The coordinates of all the atoms in the layer are fixed, which can weaken the influence of zinc crystal lattice periodicity.

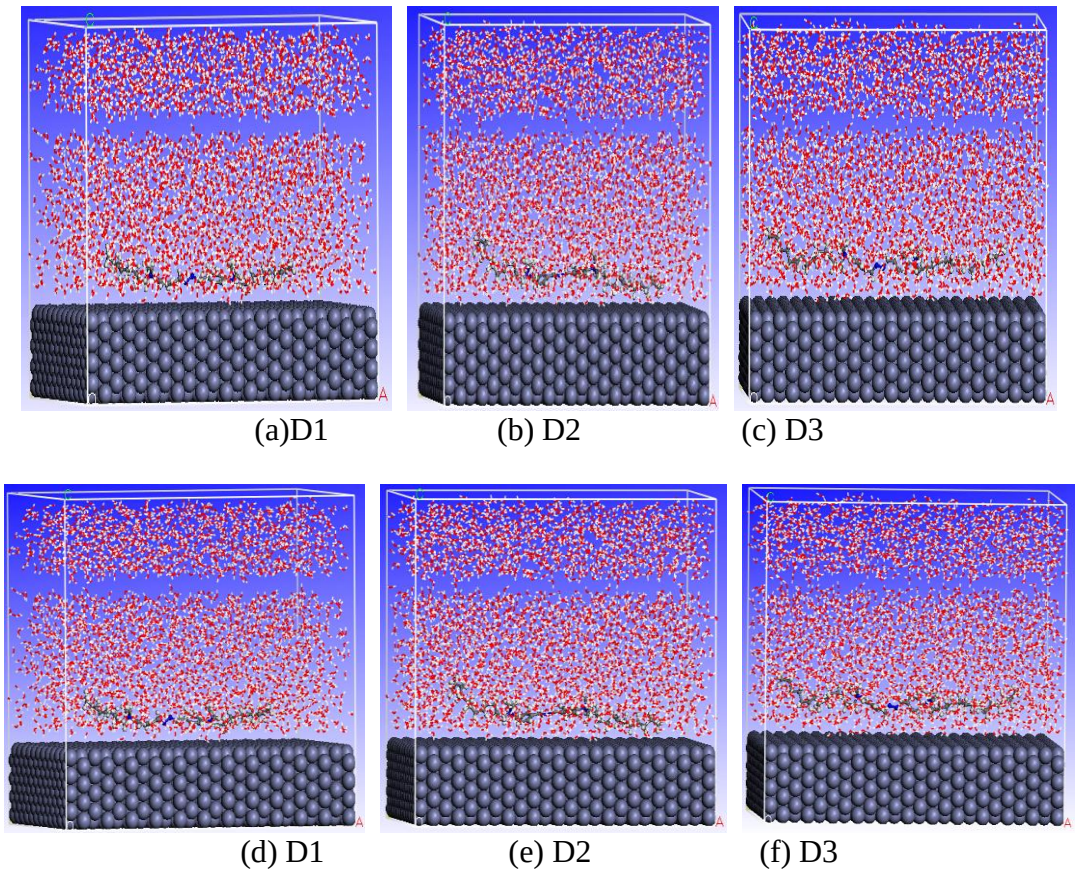

Figure 2. The initial adsorption configuration ((a), (b), (c)) and the final equilibrium adsorption configuration ((d), (e), (f)) of the surfactant molecules on Zn (1 1 0) surface in solution

Finally, Select the Build Layers in the Build module after establishing three layers. The first layer is metallic zinc supercell, the second layer is the system of 2000 water molecules, the third layer is the system of 1000 water molecules. Three layers as a whole, the surfactant molecules are placed in the second layer, and the entire calculation model[27-30] is created with size of 57.12×55.79×48.71 Å. Fig.2 shows the calculation model of the three Gemini surfactants on Zn (1 1 0) surface.

2.2. Simulation Method

The dynamics simulations mainly used Minimizer and Dynamics options in the Focrite menu. The Compass force [14] field is used to minimize the energy of the system by 5000 steps after using the Minimizer button in the Focrite menu, and then the dynamic simulation is carried out. The entire model in the process of simulation [12, 31-32] was Ensemble (NVT). The comprehensive trace file including temperature, step number and energy was obtained, which contribute to analyze the structure, mean square displacement, adsorption rate and so on. What's more, the atomic groups and

characteristic groups distance were obtained by Forcite-Analysis-Length distribution, which devoted to analyze the distance change between the atomic groups in the Gemini surfactants and distance change among the Zn (110) surface, H_2O and characteristic groups of Gemini surfactants. In this simulation experiment, the temperature is 298K, the truncation radius is 9.5 Å, the time step is 1 fs, the total dynamic simulation time is 1000 ps, and the total dynamic simulation step number is one million, a frame was output every 1000 steps.

2.3. Simulation system equilibrium

2.3.1. System balance judgment

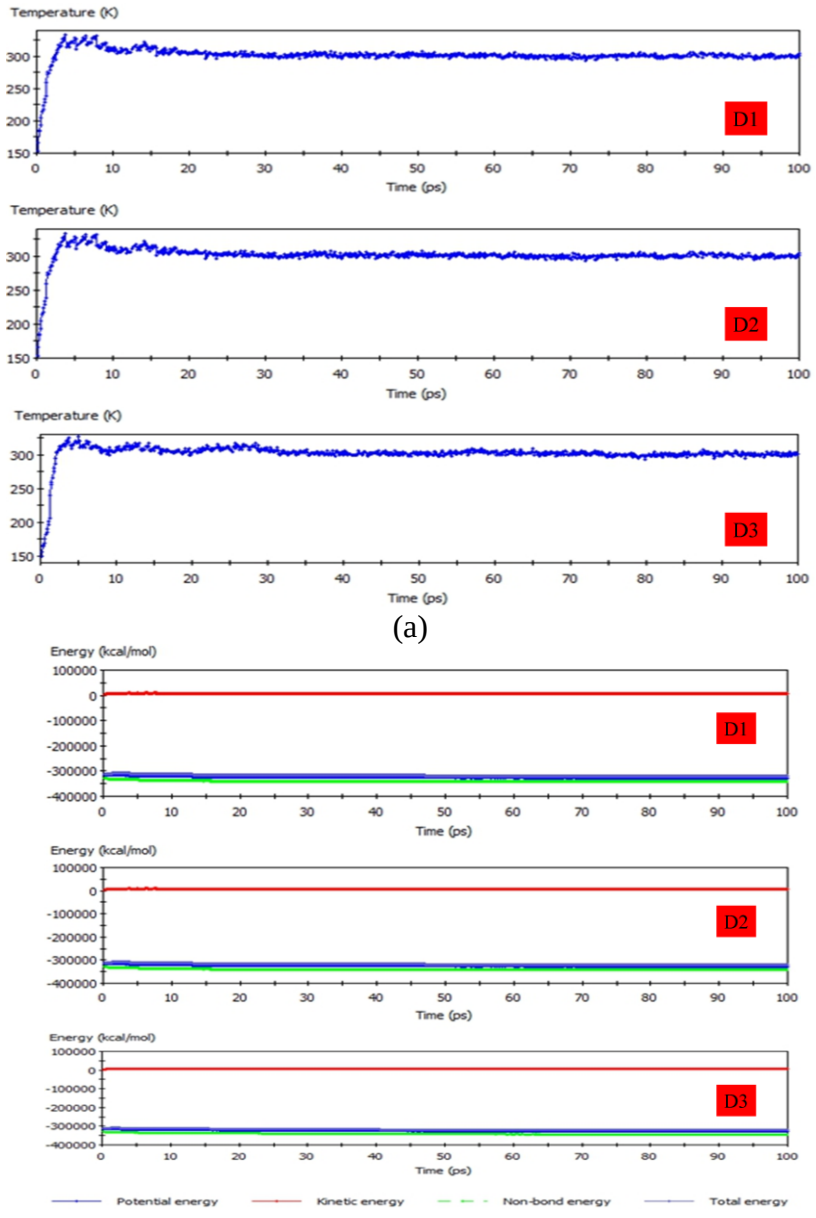

Figure 3. The temperature (a) and energy equilibrium (b) curves of three Gemini surfactants adsorbed on Zn (1 1 0) surface in solution

In the process of molecular dynamics simulation, the change of temperature, energy and time can be obtained. And when the temperature and energy of the system are stable with the calculation time, the system has reached a balance. The MD simulation on the Zn (110) surface of three Schiff base Gemini surfactant molecules in solution has reached equilibrium after 1 million steps. According to Fig.3, the system has reached the equilibrium, because the temperature, potential energy, kinetic energy, non-bond energy and total energy were all stable.

2.3.2. Adsorption energy

The adsorption energy ($E_{adsorption}$) was calculated using the following equations [26,33].

$$E_{adsorption} = E_{molecule+surface} - (E_{molecule} + E_{surface}) \quad (1)$$

where $E_{molecule}$ is the potential energy of the Schiff base Gemini surfactant molecules, $E_{surface}$ and $E_{molecule+surface}$ are the potential energy of the metal surface system without and with adsorbing Schiff base Gemini surfactant molecules, respectively.

2.3.3. Mean square displacement

The mean square displacement (MSD) was calculated using the following equations [34]:

$$MSD(t) = \left[\frac{1}{N} \sum_{1}^{N} \left(r_i(t) - r_i(0) \right)^2 \right] \quad (2)$$

$$D_\alpha = \frac{1}{6N_\alpha} \lim_{t \to \infty} \frac{d}{dt} \sum_{i=1}^{N_\alpha} \left(r_i(t) - r_i(0) \right)^2 \quad (3)$$

Where N is the number of target molecules, d is the dimension of its system, $r_i(t)$ and $r_i(0)$ are the barycentric coordinate of surfactant molecular when the time is t and 0, respectively.

3. EXPERIMENTAL DETAILS

3.1. Synthesis of inhibitors

4-(dimethylamino)benzaldehyde was reacted with three 1-Bromodecane, 1-Bromododecane, 1-Bromotetradecane to synthesize three N, N, N- dialkyl ammonium bromide benzaldehyde(L), respectively. And then the product was reaction with hydrazine hydrate to obtain the three Quaternary Ammonium Schiff base Gemini Surfactants (D1, D2, D3). The synthetic route is as follows:

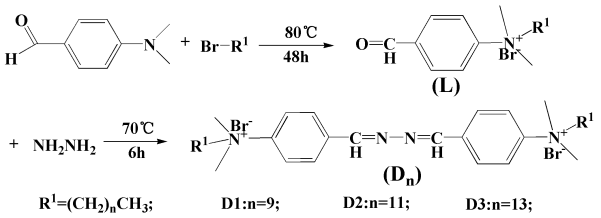

Scheme 1. The synthesis route of Surfactants

3.2. Electrolyte and electrode

3.2.1. Preparation of Electrolyte

KOH (336.66 g, 6mol) were completely dissolved in 200 mL water. The mixture was transferred into volumetric flask (1L), to prepare 6 mol/L KOH solutions. Then KOH solution (6 mol / L) was added to 25 g ZnO under magnetic stirring at room temperature, and the saturated KOH electrolyte were produced by filtering out the undissolved ZnO.

3.2.2. Pretreatment of Zinc Sheets

A big zine sheet was polished in turn by water matte papers(400 CW, 1000 CW, 1200 CW, 2000 CW) until the zinc surface became smooth and flat. Then the treated zinc sheet was polished by 1200 CW metallographic sandpaper carefully, the surface area of 1.0 × 4.0 cm^2 was washed using acetone, cleaned in distilled water in an ultrasonic bath, dried in 50℃ oven. Subsequently, Zinc sheets were wrapped in Teflon, which exposed 1.0 × 1.0 cm^2 working zinc surface [35].

3.3. Electrochemical impedance spectroscopy measurements

Electrochemical impedance spectroscopy (EIS) was determined using CHI860B electrochemical workstation (Chenhua Instruments, Beijing, China) that zinc sheet was used for a working electrode, Nickel sheet was used for an auxiliary electrode, and Hg/HgO electrode was used for a reference electrode. The surface area of 1.0 × 1.0 cm^2 nickel sheet was soaked in alkali liquor for use. All measurements were carried out at the open circuit potential stability that the test's amplitude was 5 mV, and the range of test's frequency was 0.01-1.0 × 10^5 Hz. The inhibition efficiency (η %) were calculated using the following equations [36-37].

$$\eta\% = (R_t - R^0_t)/R_t \times 100\ \% \quad (4)$$

Where R^0_t and R_t are the polarization impedance ($\Omega \cdot cm^2$) without and with the addition of Schiff base Gemini surfactants in Saturated ZnO alkaline solution, respectively.

3.4. SEM measurements

The configuration of zinc sheets corroded can be observed clearly by XSAM800 SEM. Zinc sheets are corroded lightly that the configuration become half-baked and unsmooth. The corrosion inhibition effect with surfactants can be evaluated when comparing their SEM photograph.

The experiments were divided into four groups (60 mL, per group), the one was blank group, and the other three were experimental group. The electrolyte of blank group was saturated ZnO solution with 6mol/L KOH, and the other three groups had been respectively added to three 0.7 mmol/L Schiff base Gemini surfactants (D1, D2, D3) in blank group. The surface morphology of 1.0 × 1.0 cm^2 zinc sheets was observed after burnishing, washing with distilled water, soaking with

electrolyte for 50 h, cleaning with absolute ethanol and distilled water, and drying in the ambient of vacuum. In this measurement, the area of zinc sheet is 1.0×1.0 cm^2, the magnification is 1000 times, and the accelerating voltage is 12 kV.

4. RESULTS AND DISCUSSION

4.1. EIS analysis

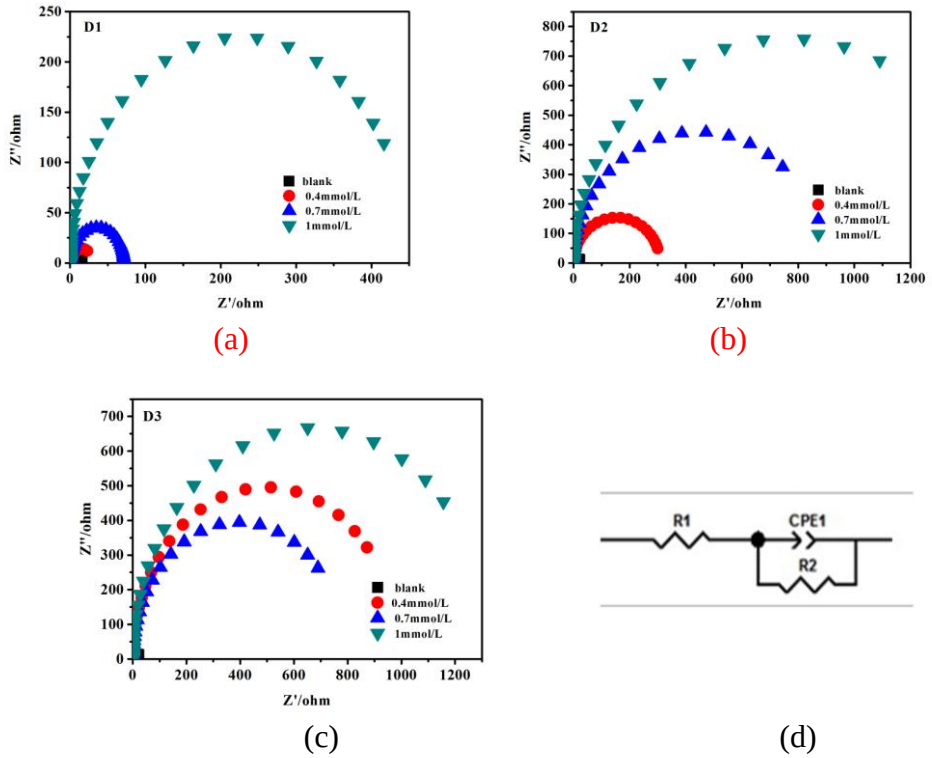

Figure 4. (a) Nyquist curves of D1 at different concentrations; (b) Nyquist curves of D2 at different concentrations; (c) Nyquist curves of D3 at different concentrations (■ 0 mmol/L, ● 0.4 mmol/L, ▲ 0.7 mmol/L, ▼1 mmol/L); (d) Equivalent circuit diagram.

Table 1. Electrochemical parameters and inhibition efficiency of zinc electrode with different concentration in the 6 mol/L KOH electrolyte of Saturated ZnO solution

Gemini surfactant	Concentration mmol/L	R1 Ω .cm^2	R2 Ω .cm^2	Cd F.cm^{-2}	η (%)
Blank	-	0.7089	52.82	0.0011610	-
D1	0.4	0.8899	314.80	0.0004123	83.22
	0.7	0.8047	380.80	0.0010930	86.13
	1.0	0.9229	744.60	0.0101300	92.90
D2	0.4	0.6232	343.30	0.0084420	84.61
	0.7	0.6177	586.20	0.0078410	90.99
	1.0	0.6866	934.45	0.0065810	94.35
D3	0.4	0.7057	548.56	0.0059290	90.34
	0.7	0.6038	900.30	0.0076870	94.13
	1.0	0.7278	1220.70	0.0046860	95.67

The EIS figures of zinc electrode with addition of different concentration inhibitors in the 6 mol/L KOH electrolyte of Saturated ZnO solution are shown in Fig. 4 (a, b, c). And the equivalent circuit diagram (Fig.4d) was used to carry out the simplest fitting, and analyze the AC impedance spectrum [38]. R1, R2, CPE1 represented solution resistance, electrochemical reaction resistance, and double layer capacitance in the equivalent circuit diagram, respectively [39]. According to equivalent circuit diagram, the experimental data of AC impedance was fitted through the Zsimpwin software. The electrochemical parameters and inhibition efficiency were listed in Table 1.

It is shown from Fig. 4 and Table 1 that the R2 values were very large compared with the R1 values [39]. And the impedance value of the zinc electrode increases with the increasing of Gemini surfactant concentration [39-41]. Compared with the blank experiment without the addition of a surfactant, the impedance value was significantly increased after adding the Gemini surfactants, which showed that the Gemini surfactants had a significant inhibition effect on the corrosion of zinc electrode. When the concentration of D1, D2, D3 is 1 mmol / L, their inhibition rate is 92.90%, 94.35% and 95.67%, respectively, so the corrosion inhibition efficiency follows the order: $\eta(D3) > \eta(D2) > \eta(D1) > \eta(blank)$.

4.2. SEM Analysis

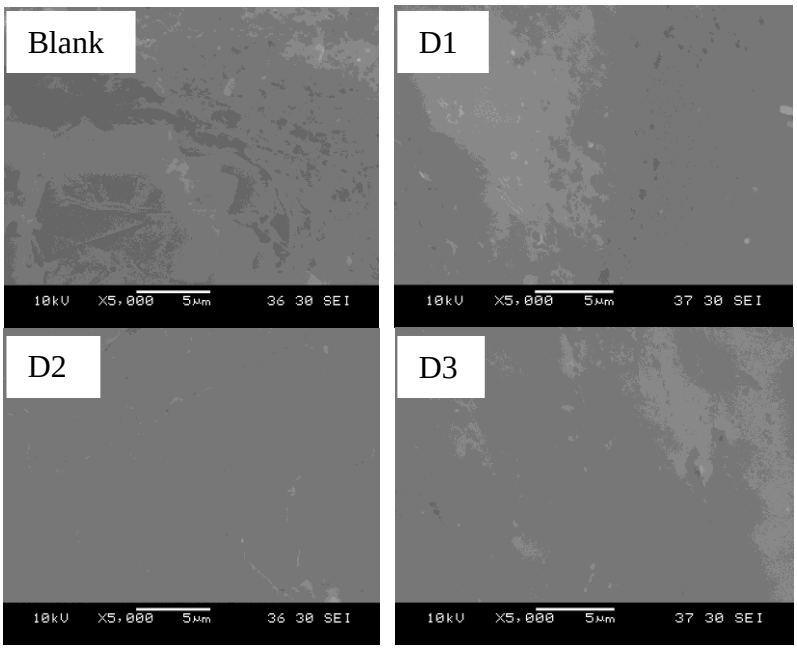

Figure 5. The SEM plots of zinc alloy electrodes with and without Gemini surfactant(D1,D2 and D3) in electrolyte

Fig. 5 shows the SEM images of zinc electrodes with and without Gemini surfactant in electrolyte. The zinc electrode was immersed in electrolyte without adding Gemini surfactant, which had obvious dendrite and signs of corrosion [42]. While adding Gemini surfactant, the zinc electrode

looked smooth and had smaller degree of corrosion. This is due to Gemini surfactant can be adsorbed on surface of the zinc electrode, and form a protective film, which can effectively inhibit corrosion of the zinc electrode [42]. It is further provided that the three kinds of Gemini surfactants have good properties of corrosion resistance and dendrite. The inhibition capacity follows the order of D3>D2>D1>blank, which is consistent with the electrochemical test results.

4.3. Equilibrium adsorption configuration and adsorption energy

4.3.1. Equilibrium adsorption configuration

The adsorption equilibrium configuration diagram of three Gemini surfactant molecules on Zn (1 1 0) surface was obtained in aqueous solution (Fig.2). In the initial adsorption configuration (Fig.2 (a), (b), (c)), the Gemini surfactants were parallel to the Zn (1 1 0) surface. The presence of water molecules had a great influence on Schiff base Gemini surfactant molecules, which could be observed after the beginning of the simulation. And the Gemini surfactant could generate slight vibration with the movement of water molecules. It indicated that there was a strong interaction between the Schiff bases Gemini surfactant molecules and water molecules, which inhibited the adsorption rate of Gemini surfactant molecules on the Zn (1 1 0) surface. The Gemini surfactant molecules begin to slowly move toward the Zn (1 1 0) surface after a period of in situ vibration. This process was influenced by the surrounding water molecules, and the Gemini surfactant molecules were always doing small vibration. The adsorption capacity between Schiff base Gemini surfactant molecules and Zn (110) surface was reduced due to the hindrance of water molecules. And the interaction of the surfactant molecules in the surrounding water molecules was relatively stable. This conclusion is consistent with previous report [43]. As the final equilibrium adsorption configuration (Fig.2 (d), (e), (f)) showed, there was not much change of three Gemini surfactant molecules on Zn (110) surface comparing with the initial adsorption configuration.

4.3.2. Adsorption energy analysis

The adsorption energy ($E_{adsorption}$) between three Schiff base Gemini surfactant molecules and the metal Zn (1 1 0) surface was tested as shown in table 2.

Table 2. The adsorption energy of three surfactants on Zn (1 1 0) surface

Molecular	D1	D2	D3
$E_{molecule+surface}$/(kcal/mol)	-33413.15	-33200.55	-33138.46
$E_{molecule}$/(kcal/mol)	-20.65	-20.75	-21.15
$E_{surface}$/(kcal/mol)	-34023.00	-34023.00	-34023.00
$E_{adsorption}$/(kcal/mol)	-630.50	-843.20	-905.69

There are the adsorption energy values of three Schiff base Gemini surfactants on Zn (1 1 0) surface in aqueous solution environment, as Table 2 shows. All adsorption energy values are negative, which indicates that the adsorption of surfactant molecules on Zn (1 1 0) surface is spontaneous [44]. Besides, the adsorption energy value of water molecules on Zn (1 1 0) surface was -44.00 kcal·mol^{-1}. And the absolute values of adsorption energy of three Schiff base Gemini surfactants molecules are significantly greater than the water molecules, indicating that the three Schiff base Gemini surfactants molecules can adsorb on the surface of zinc after expelling and replacing the water molecules. At the same time, the existence of water molecules has weakened the adsorption of Schiff base Gemini surfactant molecules in the zinc surface. In the water environment, the adsorption energy of Schiff bases Gemini surfactant follows the order E (D3)>E (D2)>E (D1). With the increase of adsorption energy, the corrosion inhibition effect becomes stronger, which is consistent with the previous test results.

4.4. Dynamic properties study

4.4.1. Adsorption rate analysis

The adsorption rate of three Schiff bases Gemini surfactant in the aqueous solution on the Zn (1 1 0) surface was studied by Calculating molecular diffusion coefficient. The mean square displacement (MSD) of three Gemini surfactants adsorbed to Zn (1 1 0) and its diffusion coefficient were showed in Fig. 6 and table 3.

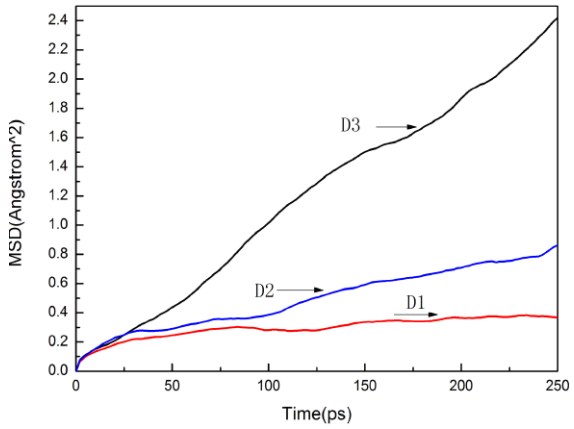

Figure 6. The MSD of three Gemini surfactants (D1, D2, D3) adsorbed to Zn (1 1 0)

Table 3. The diffusion coefficient of three surfactant molecules in solution

Gemini surfactants	D1	D2	D3
Diffusion coefficient (10^{-7}cm^2/s)	0.85	0.89	0.98

As can be seen from Fig.6, three Gemini surfactant molecules tend to move from positive direction to the interface. This may be due to the presence of van der Waals and Coulomb force in the surfactant molecules, which leads to the interaction of the chain structure and the continuous movement of the surfactant molecules [45].The Data display in Fig. 6 and table 3, the diffusion coefficient of the three Gemini surfactant molecules was small, because there were lots of water molecules in the solution, which hindered the adsorption of Gemini surfactant molecules on Zn (110) surface. The difference among the diffusion coefficient of three Gemini surfactant molecules was not very large. It was indicated that D1, D2, and D3 should have similar mobility and adsorption rate. The small differences in structure among three Gemini surfactant molecules is almost not affecting adsorption rate on Zn (110) surface. The adsorption rate of D1, D2, and D3 follows the order: D3> D2> D1. This order is consistent with their adsorption capacity on Zn (110) surface.

4.4.2. Distance change between the atomic groups in the Gemini surfactant

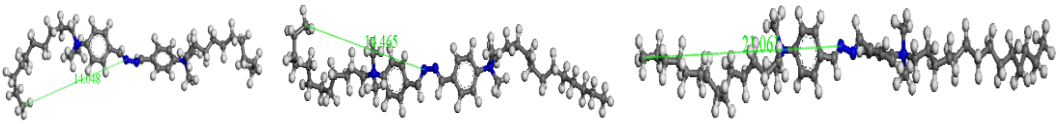

(a) D1 (b) D2 (c) D3

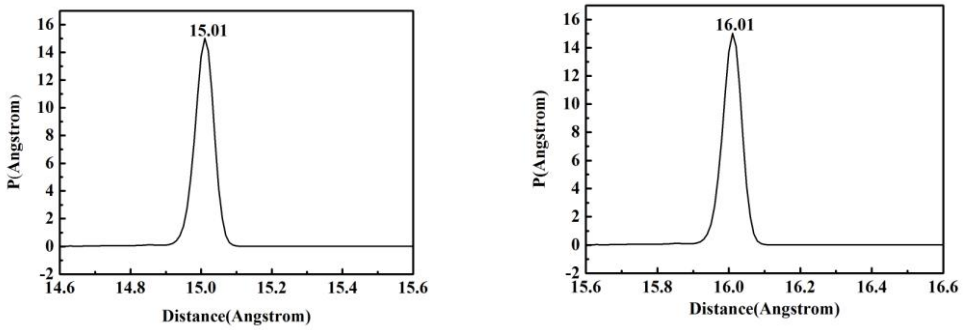

(d)D1 (e) D2

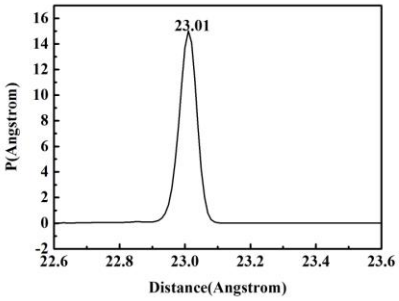

(f) D3

Figure 7. The distance before ((a), (b), (c)) and after ((d), (e), (f)) adsorption between the two groups of three Gemini surfactants

After molecular dynamics simulation, the distance changes in the process of adsorption between the atomic groups in the Gemini Surfactant were obtained by Forcite-Analysis-Length

distribution [46-47]. The calculation data was analyzed that the vertical coordinate was the distance between Gemini surfactant molecules and Zn (110) surface, the horizontal ordinate was distance between methyl on the outermost alkyl group and nitrogen atoms on the C=N double bond.

As shown in Fig. 7, there is the distance before adsorption ((a), (b), (c)) and after variation ((d), (e), (f)) between the two groups of three Gemini surfactants, respectively. The adsorption process of three Schiff base Gemini surfactants on Zn (110) surface, great changes have taken place in the distance between the two groups. After the adsorption of three Schiff base Gemini surfactants, the distance between the two groups increased about 2.0 A˚ comparing with before adsorption. The Schiff base Gemini surfactant molecules could be well adsorbed on Zn (110) surface, and then had strong adsorption energy. And it because the distance between the two groups of three Schiff base Gemini surfactants tends to elongate in the process of adsorption, the molecules essentially paralleled to adsorb on Zn (110) surface. The distance change between the atomic groups in the three Schiff base Gemini surfactants follows the order: D3> D2> D1.

4.4.3. Distance change among the Zn (110) surface, H_2O and characteristic groups of Gemini surfactants

The number density distribution function along Z axis direction of characteristic group atoms (-C=N-, -COO- and $-CH_2-CH_2-$) was calculated by Forcite-Analysis-Length distribution. The calculation data was analyzed that the vertical coordinate was the number density of characteristic group on Zn (1 1 0) surface after molecular dynamics simulation, the horizontal ordinate was the distance between the characteristic group and the Zn (1 1 0) surface.

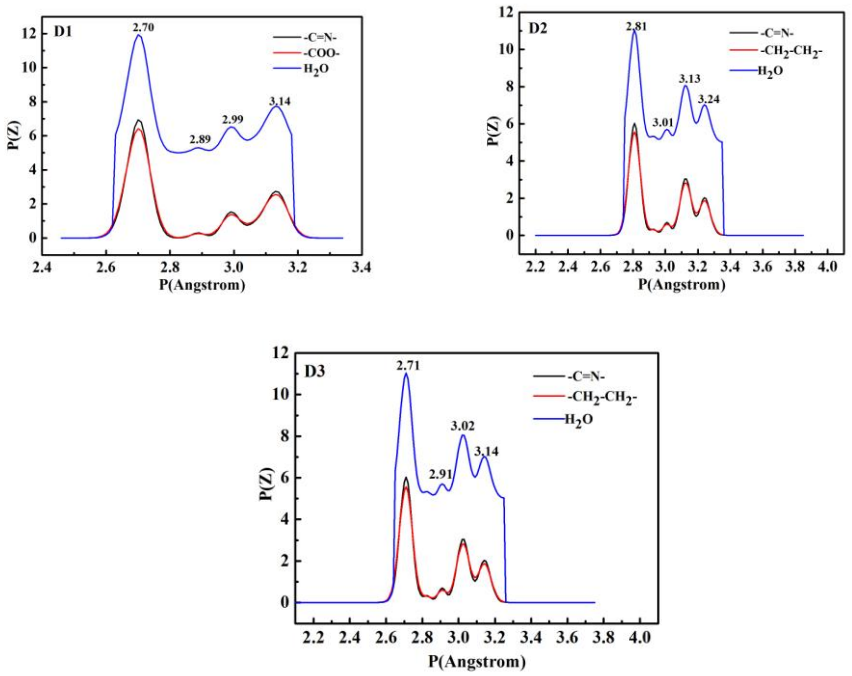

Figure 8. Change in distance among the Zn (110) surface, H_2O and characteristic groups of three Gemini surfactants

As shown in Fig. 8, the number density distribution of Gemini surfactants was very similar to the water when Gemini surfactants closed to the Zn (110) surface. The first peak is higher and narrower in all peaks. It is indicated that three Schiff base Gemini surfactants were adsorbed to the Zn (110) surface, the water number density distribution had changed. In the end, the interaction between water and Zn (110) surface was weakened owing to the interaction of two layer aqueous solution. The peak of the characteristic groups in the number density distribution curve appeared near the Zn (110) surface, and the first peak of water and density distribution in the X axis was located at the same position. This showed that the two characteristic groups of three Schiff bases Gemini surfactants all penetrated into the first layer of the aqueous solution after being adsorbed to the Zn (110) surface, which a small part of the molecules penetrated into the first layer of aqueous solution and a protective film was formed to inhibit the corrosion of zinc when most of the molecules were adsorbed to the Zn (110) surface. In summary, three Schiff base Gemini surfactants molecules were paralleled adsorbed on Zn (110) surface.

5. CONCLUSIONS

In this study, measurements include EIS and SEM were adopted to investigate the corrosion inhibition effect of three Schiff base Gemini surfactants on Zn (1 1 0) surface. The adsorption mechanism and structural changes were studied accompanying with Materials Studio 5.5.

EIS had showed that the corrosion inhibition effect of D3 were the best, which was as high as 95.67%, and the corrosion inhibition efficiency was D3> D2> D1. The SEM images showed that the corrosion inhibition capacity followed the order of D3>D2>D1. The molecular dynamics simulation showed that the equilibrium adsorption configuration of the Gemini surfactants on Zn (1 1 0) surface was obtained in the water environment. The adsorption movements of Gemini surfactant molecules on the surface of zinc metal were relatively slow.

The adsorption energy of three kinds of Gemini surfactant molecules in aqueous solution was D3>D2>D1. The bigger the adsorption energy, the stronger the inhibition effect of the molecule. All the three Schiff base Gemini surfactants molecules tended to move from the normal direction to the interface. The order of adsorption rate was D3>D2>D1, adsorption energy and adsorption rate were positively correlate.

The Schiff base Gemini surfactant molecules could be well adsorbed, and then had strong adsorption energy. The distance variation of the characteristic groups of three Schiff bases Gemini surfactants in the process of adsorption indicated a small part of the molecules penetrated into the first layer of aqueous solution and a protective film was formed to inhibit the corrosion of zinc when most of the molecules were adsorbed to the Zn (110) surface.

ACKNOWLEDGEMENTS

This work was supported by the National Nature Science Foundation of China (No. 21266006, 61661014, 61301038), the Nature Science Foundation of Guangxi Province (No. 2016GXNSFAA380109, 2015GXNSFBA139041, 2013GXNSFAA019224) and Guangxi Key Laboratory of Electrochemical and Magneto-chemical Functional Materials, Collaborative Innovation

Center for Exploration of Hidden Nonferrous Metal Deposits and Development of New Materials in Guangxi.

References

1. A. B. Y. Lim, W.J. Neo, O. Yauw, B. Chylak, C.L. Gan, Z. Chen, *Microelectro. Reliab.* 6 (2016) 155.
2. L. Guo, S. Zhu, S. Zhang, Q. He, W. Li, *Corros. Sci.* 87 (2014) 366.
3. M. K. Awad, M. R. Mustafa, M. M. Abouelnga, *Prot. Met. Phys. Chem. S.* 52 (2016) 156.
4. D. Gelman, I. Lasman, S. Elfimchev, D. Starosvetsky, Y. Ein-Eli, *J. Power Sources* 285 (2015) 100.
5. A. Mohamad, N. Mohamed, M. Yahya, R. Othman, S. Ramesh, Y. Alias, A. Arof, *Solid State Ionics* 156 (2003) 171.
6. H. Yang, Y. Cao, X. Ai, L. Xiao, *J. Power Sources* 128 (2004) 97.
7. C. W. Lee, K. Sathiyanarayanan, S. W. Eom, H. S. Kim, M. S. Yun, *J. Power Sources* 159 (2006) 1474.
8. H. M. A. El-Lateef, M. A. Abo-Riya, A. H. Tantawy, *Corros. Sci.* 108 (2016) 94.
9. M. Gorczyca, B. Korchowiec, J. Korchowiec, S. Trojan, J. Rubio-Magnieto, S.V. Luis, E. Rogalska, *J. Physical Chem. B* 119 (2015) 6668.
10. N. Poorgholami-Bejarpasi, B. Sohrabi, *Fluid Phase Equilib.* 394 (2015) 19.
11. K. F. Khaled, M. A. Amin, *Corros. Sci.* 51 (2009) 1964.
12. Y. Tang, X. Yang, W. Yang, Y. Chen, R. Wan, *Corros. Sci.* 52 (2010) 242.
13. I. B. Obot, N. O. Obi-Egbedi, *Corros. Sci.* 52 (2010) 657.
14. J. Zhang, J. Liu, W. Yu, Y. Yan, L. You, L. Liu, *Corros. Sci.* 52 (2010) 2059.
15. G. Bereket, E. Hür, C. Öğretir, *J. Mol. Struc-Theochem* 578 (2002) 79.
16. J. Cruz, T. Pandiyan, E. García-Ochoa, *J. Electroanal. Chem.* 583 (2005) 8.
17. L. M. Rodriguezvaldez, A. Martinezvillafane, D. Glossmanmitnik, *J. Mol. Struc-Theochem* 713 (2005) 65.
18. M. Lashkari, M. R. Arshadi, *Chem. Phys.* 299 (2004) 131.
19. B. Gómez, N. V. Likhanova, M. A. Domínguez Aguilar, O. Olivares, J.M. Hallen, J.M. Martínezmagadán, *J. Phys. Chem. A* 109 (2005) 8950.
20. Y. Hui, S. Yuan, S. Zeng, M. Niu, *Appl. Surf. Sci.* 349 (2015) 163.
21. X. Wang, L. Liu, P. Wang, W. Li, J. Zhang, Y. G. Yan, *Ind. Eng. Chem. Res.* 53 (2014) 16785.
22. Y. Wang, H. B. Yi, H. J. Li, Q. Dai, Z. W. Cao, Y. Lu, *Acta Phys-Chim Sin.* 31 (2009) 1035.
23. H. Zhao, X. Zhang, L. Ji, H. Hu, Q. Li, *Corros. Sci.* 83 (2014) 261.
24. D. Daoud, T. Douadi, H. Hamani, S. Chafaa, M. Al-Noaimi, *Corros. Sci.* 94 (2015) 21.
25. S. Deng, X. Li, X. Xie, *Corros. Sci.* 80 (2014) 276.
26. K. F. Khaled, *Electrochim. Acta* 55 (2010) 5375.
27. J. Ren, J. Zhao, Z. Dong, P. Liu, *Appl. Surf. Sci.* 346 (2015) 84.
28. Z. Amjad, J. P. Hooley, *Tenside Surfact. Det.* 31 (1994) 12.
29. I. Drela, P. Falewicz, S. Kuczkowska, *Water Res.* 32 (1998) 3188.
30. A. Y. Musa, R. T. T. Jalgham, A. B. Mohamad, *Corros. Sci.* 56 (2012) 176.
31. K. F. Khaled, *Appl. Surf. Sci.* 255 (2008) 1811.
32. S. Xia, M. Qiu, L. Yu, F. Liu, H. Zhao, *Corros. Sci.* 50 (2008) 2021.
33. K. F. Khaled, *Corros. Sci.* 52 (2010) 3225.
34. B. Liu, Y. Lian, Z. Li, G. Chen, *Acta Chim. Sinica* 72 (2014) 942.
35. D. A. Teixeira, M. A. G. Valente, A. V. Benedetti, G. T. Feliciano, S. C. da Silva, C. S. Fugivara, *J. Braz. Chem. Soc.* 26(2014)57.
36. B. P. Markhali，R. Naderi，M. Mahdavian，M. Sayebani，S. Y. Arman, *Corros. Sci.* 75 (2013) 269.

37. V. M. Abbasov, H. M. A. El-Lateef, L. I. Aliyeva, I. T. Ismayilov, E. E. Qasimov, M. M. Narmin, V. M. Abbasov, L. I. Aliyeva, I. T. Ismayilov, E. E. Qasimov, *J. Korean Chem. Soc.* 57 (2013) 25.
38. I. Ahamad, R. Prasad, M. A. Quraishi, *Corros. Sci.* 52 (2010) 933.
39. M. Behpour, S. M. Ghoreishi, N. Mohammadi, N. Soltani, M. Salavati-Niasari, *Corros. Sci.* 52 (2010) 4046.
40. K. F. Khaled, *Mater. Chem. Phys.* 112 (2008) 290.
41. K. F. Khaled, *J. Solid State Electrochem.* 13 (2009) 1743.
42. M. Yadav, S. Kumar, D. Behera, I. Bahadur, D. Ramjugernath, *Int. J. Electrochem. Sci.*, 9 (2014) 5235.
43. V. F. Ekpo, P. C. Okafor, U. J. Ekpe, E. E. Ebenso, *Int. J. Electrochem. Sci.* 6 (2011) 1045.
44. M. K. Awad, M. R. Mustafa, M. M. Abo-Elnga, *J. Mol. Struct. Theochem* 959 (2010) 66.
45. S. Q. Hu, A. L. Guo, Y. G. Yan, X. L. Jia, Y. F. Geng, W. Y. Guo, *Comput. Theor. Chem.* 964 (2011) 176.
46. A. Kuehnle, *Chem. Inform.* 14 (2009) 157.
47. Z. Xu, S. L. Yuan, H. Yan, C. B. Liu, *Colloid. Surface. A* 380 (2011) 135.